# Controls on the 87Sr/86Sr ratios of carbonates in the Garhwal Himalaya, Headwaters of the Ganges

# Controls on the $^{87}Sr/^{86}Sr$ Ratio of Carbonates in the Garhwal Himalaya, Headwaters of the Ganges

*M. J. Bickle, N. B. W. Harris,[1] J. M. Bunbury, H. J. Chapman, I. J. Fairchild,[2] and T. Ahmad[3]*

*Department of Earth Sciences, Downing Street, Cambridge CB2 3EQ, United Kingdom (e-mail: MB72@esc.cam.ac.uk)*

**ABSTRACT**

The episodic variation of the seawater $^{87}Sr/^{86}Sr$ ratio has been attributed to either variations in the Sr flux or the Sr-isotopic composition of the riverine-dissolved load derived from weathering of the continental crust. The discovery that Himalayan rivers are characterized by high concentrations of dissolved Sr concentrations with high $^{87}Sr/^{86}Sr$ ratios has raised the possibility that collisional orogens play a critical role in moderating the variations in seawater $^{87}Sr/^{86}Sr$ ratios. Here we describe Himalayan carbonates and calc-silicates from Garhwal, the headwaters of the Ganges, with extreme $^{87}Sr/^{86}Sr$ ratios (>1.0). Elevated Sr-isotope ratios result from exchange with Rb-rich silicate material during both Himalayan and pre-Himalayan metamorphic episodes, and the carbonates contribute a significant fraction to the Ganges $^{87}Sr$ flux. Particularly elevated $^{87}Sr/^{86}Sr$ ratios are found in calc-silicates from the Deoban Formation of the Lesser Himalaya. A detailed traverse of shales and calc-silicates from this unit confirms that carbonate horizons have increased $^{87}Sr/^{86}Sr$ ratios as a result of isotopic exchange over length scales of 10–30 cm. We conclude that metamorphism of carbonates may cause elevation of their $^{87}Sr/^{86}Sr$ ratios and that uplift of metamorphosed carbonates may be a consequence of collisional orogens, which contributes to the elevation of seawater $^{87}Sr/^{86}Sr$ ratios.

## Introduction

The significance of the variations in the global riverine $^{87}Sr$ flux implied by the seawater $^{87}Sr/^{86}Sr$ curve is controversial (Raymo and Ruddiman 1992; Richter et al. 1992; Quade et al. 1997). The changes in the riverine $^{87}Sr$ flux may reflect variation in silicate weathering rates, a change in the Sr content of the source rocks, a change in the $^{87}Sr/^{86}Sr$ ratios of the Sr derived from silicate weathering, or possibly, a variable contribution from carbonates with elevated $^{87}Sr/^{86}Sr$ ratios. Which of these mechanisms dominates is important because variation in silicate weathering fluxes would imply correspondingly large variations in global $CO_2$ degassing rates (e.g., Bickle 1996), whereas changes in the mean $^{87}Sr/^{86}Sr$ of components contributing to the riverine Sr flux might imply some long-term tectonic control on seawater $^{87}Sr/^{86}Sr$ ratios.

Raymo et al. (1988) suggested a connection between the sudden and monotonic increase in the seawater $^{87}Sr/^{86}Sr$ ratio from 40 Ma and the uplift and erosion of the Himalayan mountain chain, which commenced about the same time. Modeling by Richter et al. (1992) and most recently by Galy et al. (1999) and English et al. (2000) has confirmed the significance of the fluxes from rivers draining the Himalayas and Tibet to the post-Eocene rise in the seawater $^{87}Sr/^{86}Sr$ ratio. Himalayan rivers may have a disproportionate effect on seawater $^{87}Sr/^{86}Sr$ ratios because they have both elevated $^{87}Sr/^{86}Sr$ ratios and high Sr contents (Edmond 1992). The main Himalayan metasedimentary units are all older than ~500 Ma and are characterized by high $^{87}Sr/^{86}Sr$ silicate minerals (Krishnaswami et al. 1992), but silicate weathering characteristically generates water with low Sr concentrations but high $^{87}Sr/^{86}Sr$ (Edmond 1992). Transfer of Sr from less easily weathered Rb-rich minerals, such as micas, to more easily

Manuscript received September 19, 2000; accepted April 12, 2001.

[1] Department of Earth Sciences, Open University, Milton Keynes MK7 6AA, United Kingdom.

[2] School of Earth Sciences and Geography, Keele University, Staffs ST5 5BG, United Kingdom.

[3] Institute of Himalayan Geology, Dehra Dun 248001, Uttar Pradesh, India.

[The Journal of Geology, 2001, volume 109, p. 737–753]  0022-1376/2001/10906-0004$01.00

weathered Ca-silicate phases, such as feldspars, by dehydration or melting mineral reactions is one possible cause of the enhanced riverine $^{87}Sr$ flux (Edmond 1992; Harris 1995). However, Palmer and Edmond (1992) suggested that the relatively young Himalayan metamorphism had led to exchange between $^{87}Sr$-rich silicate minerals and carbonate, yielding an easily weathered, high $^{87}Sr/^{86}Sr$, Sr-rich source. The existence of such high $^{87}Sr/^{86}Sr$ carbonates has been confirmed by Derry and France-Lanord (1996), Quade et al. (1997), Blum et al. (1998), Harris et al. (1998), Singh et al. (1998), and English et al. (2000). The relative contributions to riverine fluxes from carbonate dispersed in silicate rocks and the various carbonate rocks are still disputed (Blum et al. 1998; Singh et al. 1998; Galy et al. 1999; English et al. 2000). However, all these studies of river chemistry conclude that a significant fraction of the Sr is derived from carbonate rocks; therefore, it is important to know the geochemical characteristics of the carbonate rocks and why their $^{87}Sr/^{86}Sr$ ratios are elevated.

Previous studies on Himalayan river chemistry have focused on the variations of $^{87}Sr/^{86}Sr$ ratios in the river waters. Here we review controls on the Sr-isotopic composition of carbonate rocks from the High Himalayan Crystalline Series and the Lesser Himalayas in the Garhwal Himalaya, headwaters of the Ganges. We present chemical analyses of some carbonate rocks with extraordinarily high $^{87}Sr/^{86}Sr$ ratios and assess the timing and scale of Sr isotopic exchange responsible for the elevation of the carbonate $^{87}Sr/^{86}Sr$ ratios. We show that the $^{87}Sr/^{86}Sr$ ratios of the carbonate rocks were elevated by exchange between silicate and carbonate minerals during both Himalayan and pre-Himalayan metamorphic episodes. Since carbonate rocks contribute to the riverine Sr flux, uplift and erosion of such altered rocks by collisional orogens may have had an impact on seawater $^{87}Sr/^{86}Sr$ ratios.

## Controls on Riverine $^{87}Sr/^{86}Sr$ Ratios: Bedrock Composition

Because dissolved riverine Sr is derived from weathering of both silicate and carbonate minerals, the relative contributions from each must be known if riverine $^{87}Sr/^{86}Sr$ isotope ratios are to be related to the alkalinity flux derived from silicate weathering. Silicate sedimentary, metamorphic, and granitic igneous rocks have high Rb/Sr ratios and rapidly evolve high $^{87}Sr/^{86}Sr$ ratios, although the mean $^{87}Sr/^{86}Sr$ of the sediment mass is moderated by processes during sedimentary reworking (e.g., Bickle 1994). However, the $^{87}Sr/^{86}Sr$ ratio of Sr released by weathering may be controlled by the $^{87}Sr/^{86}Sr$ ratio of the more easily weathered minerals in addition to the small (and poorly documented) fraction of easily exchangeable Sr located along grain boundaries or in damaged mineral lattices. The Himalayan orogen has exhumed unusually old metasedimentary rocks that have evolved to high $^{87}Sr/^{86}Sr$ ratios and, in the High Himalayan Crystalline Series, have been metamorphosed to upper-amphibolite facies, resulting in the transfer of Sr to more easily weathered plagioclase (Harris 1995).

Pure carbonate rocks characteristically contain high Sr and very low Rb. The mean Rb/Sr ratio of the carbonate rock reservoir is too low (Rb/Sr, ~0.02) to cause a significant increase in the $^{87}Sr/^{86}Sr$ ratio between burial and exhumation, and the initial $^{87}Sr/^{86}Sr$ ratios should be close to that of contemporary seawater. Seawater $^{87}Sr/^{86}Sr$ ratios have probably varied between ~0.7033 in the Archean, to 0.7055 in the early Proterozoic, to 0.706–0.707 by the late Precambrian (Veizer 1989; Jacobsen and Kaufman 1999), the periods over which the Lesser Himalayan Series and High Himalayan Crystalline Series rocks sampled here were deposited.

Elevation of carbonate $^{87}Sr/^{86}Sr$ ratios can occur during diagenetic processes of dolomitization or during metamorphism. The low Sr abundances of Himalayan dolomites (which constitute the majority of Himalayan carbonates) are indicative of dolomitization of diagenetic limestones (diagenetic limestones are characterized by low Sr due to the lower Sr/Ca ratio in calcite compared with aragonite). Late diagenetic dolomitization commonly occurs in limestones bounding clay beds (Yoo et al. 2000) and may be related to the release of Mg from the conversion of smectite to illite during burial. Globally, dolomites with $^{87}Sr/^{86}Sr$ ratios of 0.708–0.716 are quite common (Banner 1995), and this elevation of Sr isotope ratios probably occurs during the dolomitization. Many of the Himalayan carbonate rocks are impure and may have exchanged Sr between Rb-poor carbonate minerals and Rb-rich, and thus high $^{87}Sr/^{86}Sr$ silicate minerals, if subjected to even low-grade metamorphism. In addition, the fluid phase in metamorphic rocks may cause advective or diffusive exchanges of Sr between silicate and carbonate rocks over distances up to several meters (e.g., Bickle and Chapman 1990; Bickle et al. 1995, 1997). For the Himalayan carbonates, many of which have high Rb/Sr ratios, it is important to estimate (1) whether the increase in $^{87}Sr/^{86}Sr$ ratio is supported by $^{87}Rb$ decay since deposition, (2) the nature of the process that caused exchange between silicate and carbonate

minerals, and (3) when the process occurred. This is necessary to estimate the initial $^{87}Sr/^{86}Sr$ ratio of the carbonate.

## The Garhwal Himalaya

The Garhwal Himalaya forms the segment between the Nepal and Zanskar Himalaya (fig. 1). From northwest to southeast, the Himalaya comprises five main tectonic units: (1) the Mesozoic trans-Himalayan batholith on the margin of the northern continent; (2) the Indus-Tsangpo suture zone with fragments of the oceanic crust from the ocean basin; (3) the Tibetan Sedimentary Series deposited on the northern edge of the Indian subcontinent; (4) the High Himalayan Crystalline Series comprising deeply buried metamorphic rocks emplaced by the Main Central Thrust and originally probably basement to, or the basal part of, the Tibetan Sedimentary Series; and (5) the Lesser Hima-

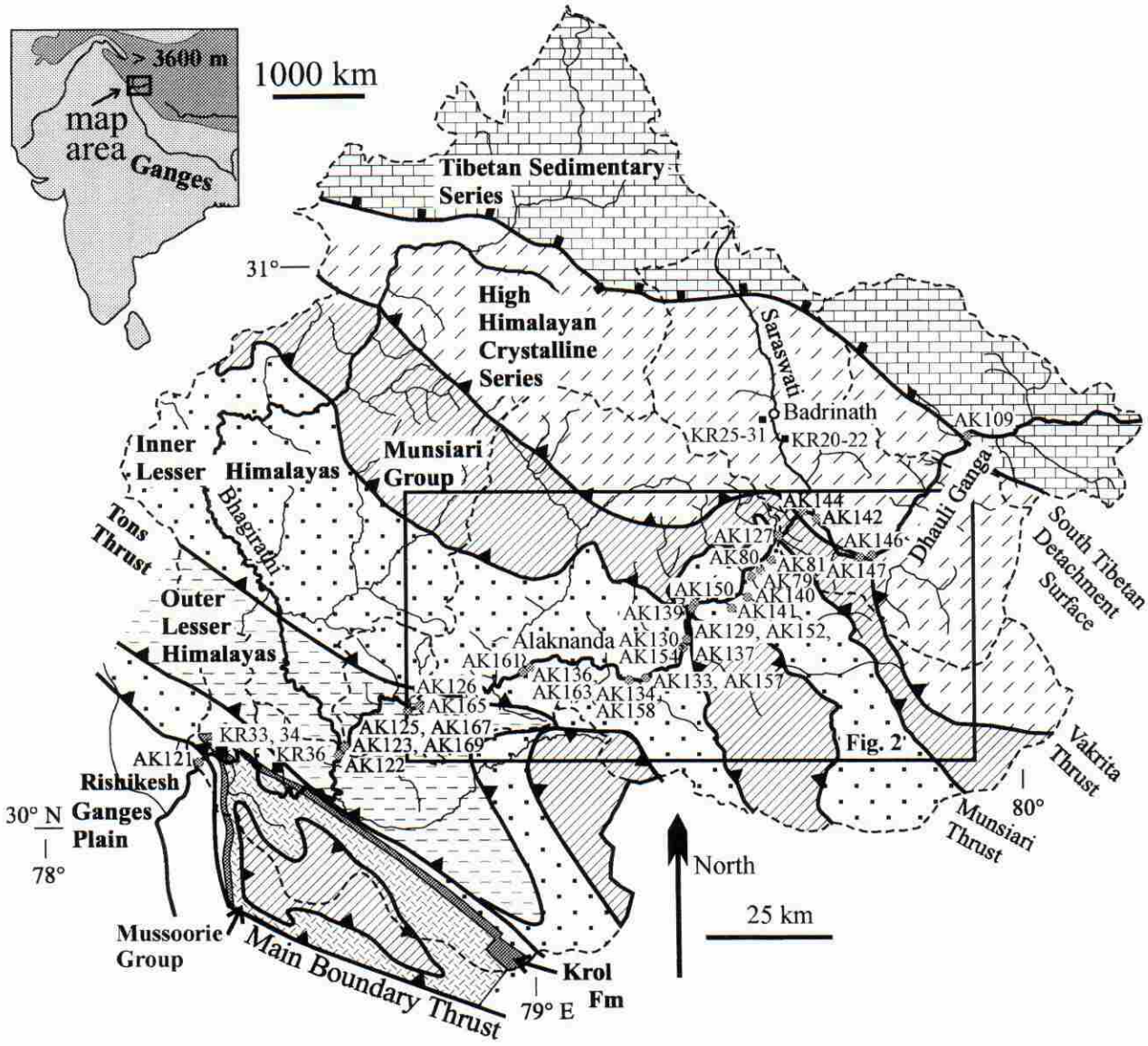


**Figure 1.** Geological map of catchments of Ganges headwaters in the Garhwal Himalaya after Valdiya (1980), Metcalfe (1990), Thakur and Rawat (1992), and Prince (1999), with classification of Lesser Himalayan units after Valdiya (1980) and Ahmad et al. (2000). River catchment boundaries are shown as dashed lines. Rock sample sites (prefix *KR*) from Badrinath traverse and Outer Lesser Himalayas and water sample sites (prefix *AK*) are shown.

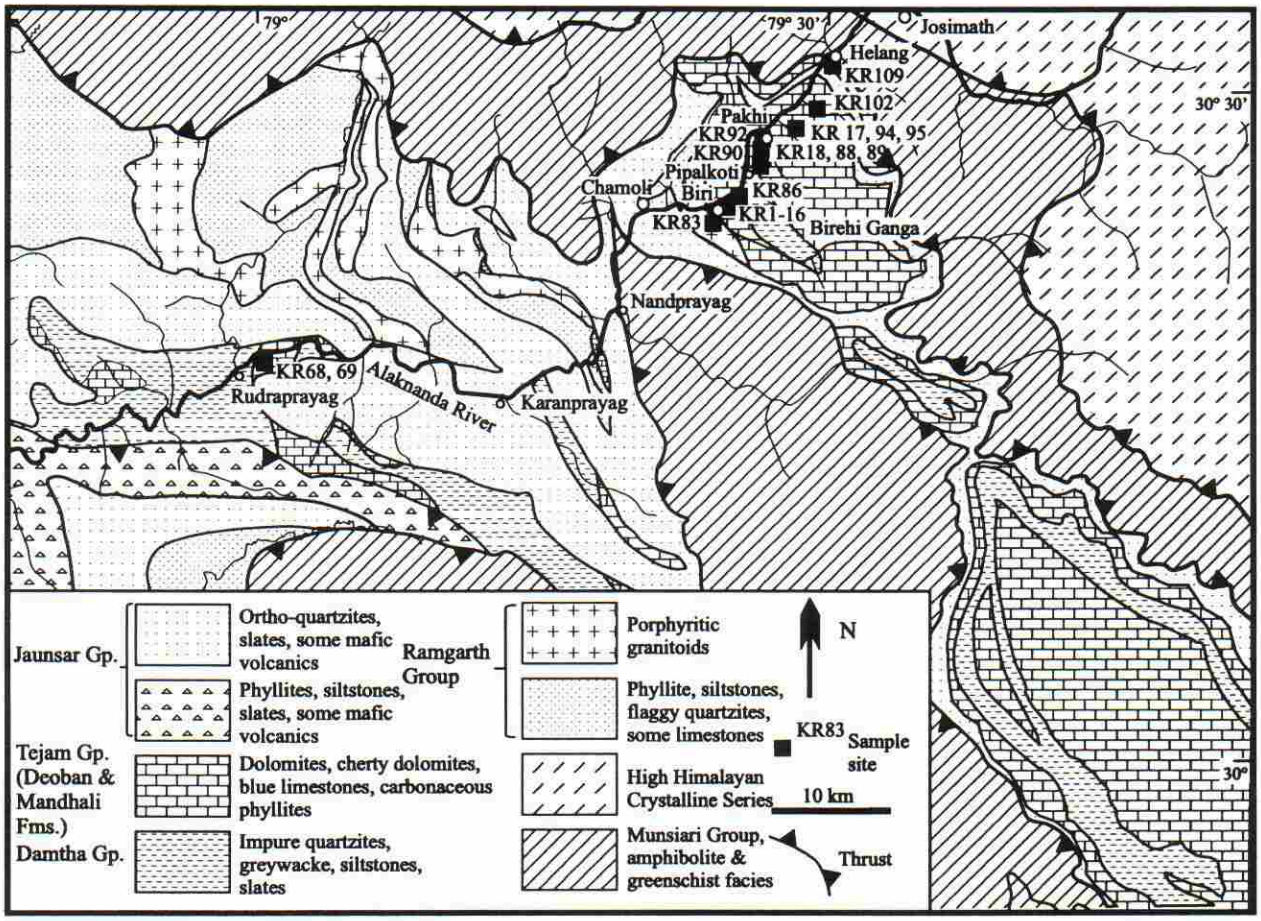


**Figure 2.** Detailed map of geology between Josimath and Rudraprayag after Valdiya (1980) showing bedrock sample localities. Only the major thrusts are shown. Map location shown in figure 1.

layan Series, which includes up to 1.8 Ga or older low-grade metasediments. The Lesser Himalayan Series overthrusts synorogenic foreland basin sediments of the Sub-Himalayan Sequence to the south. The High Himalayan Crystalline Series underlies the highest mountains that cause a rain shadow for the Tibetan Plateau. As a result of antecedent drainage, the main rivers eroding the Himalayas initially flow across the Tibetan Plateau or Tibetan Sedimentary Series before cutting through the High Himalayan Crystalline Series and the Lesser Himalayan Series to the foreland basin. The High Himalayan Crystalline Series supplies ~80% of the material transported to the Bengal Fan (Derry and France-Lanord 1996). Much of the rest of the detritus is probably supplied by the lower-elevation Lesser Himalaya.

The High Himalaya Crystalline Series comprises high-grade gneisses, schists, and granites, with limited carbonate and calc-silicate rocks. The sediments were derived from a source with a depleted mantle Nd model age of 1800–2000 Ma and were subsequently metamorphosed at ~500 Ma. Himalayan high-grade metamorphism subsequently occurred from the Early Miocene (~35–20 Ma; Vance and Harris 1999) with the youngest exposed garnet-grade rocks with peak metamorphic ages as young as ~6 Ma (Harrison et al. 1997).

The Lesser Himalayan Series comprises mainly low-grade schists and phyllites (sub-kyanite grade) with intercalated calc-silicates and massive dolomites and minor mafic and granitic igneous rocks. The Lesser Himalayan Series is cut by a series of thrusts. The generally unfossiliferous nature of the Precambrian lithologies, combined with their intercalation with some fossiliferous Phanerozoic strata, has led to considerable uncertainty about their stratigraphic and structural relationships and

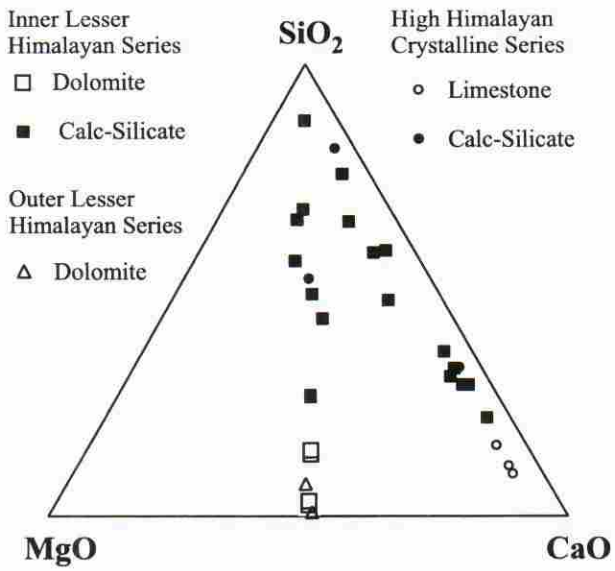


**Figure 3.** Triangular plot of $SiO_2$-MgO-CaO (mol %) of carbonate rocks from the Garhwal Himalaya. Note that the carbonate phase is either dominantly calcite or dominantly dolomite but with a complete range from pure limestone or dolomite through siliceous calc-silicate to carbonate-poor siliceous sediments.

ages (Valdiya 1980; Srivastava and Mitra 1994). Isotopic studies show that much of the sequence has ~2500–2900-Ma depleted-mantle model Nd ages ($\epsilon_{Nd}$, ~−25), was deposited after 1.9 Ga (determined from detrital zircon ages), and was metamorphosed at 1800 Ma and possibly 500 Ma (France-Lanord et al. 1993; Oliver et al. 1995; Parish and Hodges 1996; Ahmad et al. 2000). Nd isotopic analyses on rocks from Garhwal by Ahmad et al. (2000) have revealed a more complicated origin for the Lesser Himalayan Series (fig. 1), with an external unit (the Outer Lesser Himalaya) characterized by younger Nd isotopic model ages (~1900–2200 Ma), less negative $\epsilon_{Nd}$ (~−17.5), and geochemistry similar to the High Himalayan Crystalline Series. The phyllites and siltstones of the Outer Lesser Himalaya may be equivalents of the High Himalayan Crystalline Series that have escaped high-grade metamorphism during the Himalayan orogeny. The Inner and Outer Lesser Himalaya are separated by the Tons Thrust (fig. 1). The extent of Himalayan metamorphism in the Lesser Himalayan Series is variable. The Munsiari Group, identified as Lesser Himalayan Series by old model ages and negative $\epsilon_{Nd}$ (−23 to −28), exhibits inverted metamorphic isograds of garnet and staurolite grade. It outcrops as the footwall to the Main Central Thrust (MCT) and as a series of structurally high klippen overlying Inner as well as Outer Lesser Himalayan units (fig. 1). The Ramgarh Group (fig. 2) is also metamorphosed up to garnet grade. The other Lesser Himalayan units are chlorite or biotite grade of uncertain age, although we have identified phlogopite in calc-silicates of the Deoban Formation that postdates crenulated white-mica fabrics of probable MCT age.

We have analyzed bedrock samples from the High Himalayan Crystalline Series and Lesser Himalayan Series including two detailed traverses of intercalated carbonates, calc-silicates, and silicates in the High Himalayan Crystalline Series and Inner Lesser Himalayas (figs. 1, 2). The sample set ranges from impure limestones to calcitic calc-silicates in the High Himalayan Crystalline Series, dolomites to calcitic and dolomitic calc-silicates in the Inner Lesser Himalayas, and massive dolomites in the Outer Lesser Himalayas (fig. 3). We also present analyses of dissolved Sr in the Alaknanda River between Joshimath and Rishikesh sampled at a time of high flow in 1998.

## Analytical Methods

Major-element compositions of rock samples (table 1) were determined by wavelength-dispersive x-ray fluorescence (XRF) spectrometry on fused discs at the Open University using a 3-kW Rh-anode end-window x-ray tube. Element intensities were corrected for background and known peak-overlap interferences by using a drift monitor. Matrix corrections employed the empirical Traill-Lachance procedure. Rb and Sr were analyzed on powder pellets by a separate program using long count times to ensure Rb/Sr ratios were precise to better than 2% ($2\sigma$).

$^{87}Sr/^{86}Sr$ ratios of rock samples (tables 2, 3) were analyzed at Cambridge as described by Ahmad et al. (2000) following dissolution using HF-$HNO_3$, $HNO_3$, and HCl stages in Teflon bombs at 180°C. $^{87}Sr/^{86}Sr$ ratios are normalized to $^{87}Sr/^{86}Sr = 0.1194$. Water samples were filtered through 0.1 $\mu$m cellulose nitrate filters, acidified on-site with twice quartz-distilled HCl to give a pH of ~2, and kept in 30-mL polypropylene bottles. $^{87}Sr/^{86}Sr$ measurements on water samples were made on Sr separated from 5 mL and processed through a cation-exchange column. Sr blanks on both rock and water samples were less than 1‰ of the sample size. Analyses of NBS987 gave $^{87}Sr/^{86}Sr = 0.710270 \pm 0.0000018$ ($2\sigma$) over the period of the analyses. Isochron regression calculations were made after York (1969).

Carbonate fractions were leached from silicates

**Table 1.** Major-Element Analyses of Carbonate Whole-Rock Samples

| Sample | East[a] | North | $SiO_2$ | $TiO_2$ | $Al_2O_3$ | $Fe_2O_3$ | MnO | MgO | CaO | $Na_2O$ | $K_2O$ | $P_2O_5$ | LOI[b] | Total | Ca#[c] |
|---|---|---|---|---|---|---|---|---|---|---|---|---|---|---|---|
| Badrinath traverse (HHCS): | | | | | | | | | | | | | | | |
| KR25 | 79°29.37′ | 30°44.64′ | 74.00 | .59 | 12.11 | 3.79 | .01 | 1.19 | 1.37 | 5.09 | .71 | .15 | .52 | 99.53 | .453 |
| KR26 | 79°29.37′ | 30°44.64′ | 50.69 | .17 | 3.67 | 2.83 | .11 | 14.96 | 21.40 | .75 | .58 | .06 | 4.29 | 99.51 | .507 |
| KR27 | 79°29.37′ | 30°44.64′ | 10.26 | .10 | 1.88 | 1.24 | .06 | 2.54 | 46.50 | .64 | .08 | .04 | 36.50 | 99.85 | .929 |
| KR28 | 79°29.37′ | 30°44.64′ | 22.02 | .21 | 3.76 | 1.94 | .08 | 2.06 | 39.02 | 1.80 | .26 | .06 | 28.98 | 100.18 | .932 |
| KR29 | 79°29.37′ | 30°44.64′ | 7.24 | .06 | 1.20 | 1.86 | .07 | 2.44 | 48.54 | .32 | .12 | .03 | 38.56 | 100.44 | .935 |
| KR30 | 79°29.37′ | 30°44.64′ | 5.86 | .06 | 1.12 | 1.70 | .08 | 2.34 | 49.30 | .28 | .08 | .02 | 39.76 | 100.61 | .938 |
| KR31 | 79°29.37′ | 30°44.64′ | 63.82 | .54 | 10.59 | 3.37 | .05 | 1.83 | 10.39 | 2.44 | 2.58 | .15 | 4.21 | 99.96 | .803 |
| Biri traverse (Deoban Fm. ILHS): | | | | | | | | | | | | | | | |
| KR1 | 79°24.8′ | 30°24.2′ | 40.50 | .34 | 8.16 | 2.99 | .07 | 2.56 | 22.58 | .99 | 1.71 | .11 | 19.95 | 99.96 | .864 |
| KR2 | 79°24.8′ | 30°24.2′ | 14.00 | .10 | 2.14 | 1.12 | .03 | 2.04 | 42.84 | .54 | .42 | .03 | 36.38 | 99.64 | .938 |
| KR3 | 79°24.8′ | 30°24.2′ | 21.22 | .12 | 2.44 | 1.56 | .03 | 3.08 | 37.92 | .40 | .54 | .05 | 33.36 | 100.73 | .899 |
| KR4 | 79°24.8′ | 30°24.2′ | 19.00 | .12 | 2.64 | 1.20 | .04 | 2.56 | 39.48 | .42 | .64 | .04 | 33.98 | 100.13 | .917 |
| KR5 | 79°24.8′ | 30°24.2′ | 24.14 | .19 | 4.14 | 1.74 | .03 | 2.40 | 35.38 | .52 | 1.04 | .06 | 30.44 | 100.08 | .914 |
| KR6 | 79°24.8′ | 30°24.2′ | 21.36 | .13 | 3.16 | 1.48 | .03 | 2.48 | 37.82 | .50 | .72 | .05 | 32.56 | 100.29 | .917 |
| KR7 | 79°24.8′ | 30°24.2′ | 19.42 | .12 | 3.26 | 1.24 | .03 | 1.86 | 39.58 | .74 | .70 | .04 | 33.40 | 100.39 | .939 |
| KR8 | 79°24.8′ | 30°24.2′ | 38.94 | .33 | 9.65 | 2.49 | .08 | 3.67 | 20.65 | .79 | 2.49 | .06 | 20.66 | 99.80 | .802 |
| KR9 | 79°24.8′ | 30°24.2′ | 46.99 | .33 | 7.71 | 2.08 | .06 | 4.55 | 16.62 | .74 | 2.03 | .05 | 18.71 | 99.87 | .725 |
| KR10 | 79°24.8′ | 30°24.2′ | 33.66 | .29 | 6.46 | 2.68 | .10 | 4.58 | 24.86 | .62 | 1.66 | .07 | 25.05 | 100.03 | .796 |
| KR11 | 79°24.8′ | 30°24.2′ | 32.64 | .16 | 3.86 | 1.68 | .07 | 4.36 | 28.28 | .72 | .86 | .05 | 27.31 | 99.98 | .824 |
| KR12 | 79°24.8′ | 30°24.2′ | 12.00 | .09 | 1.84 | .84 | .03 | 2.38 | 44.16 | .56 | .30 | .04 | 37.49 | 99.73 | .930 |
| KR13 | 79°24.8′ | 30°24.2′ | 20.60 | .14 | 3.58 | 1.40 | .04 | 3.22 | 37.14 | .50 | .78 | .05 | 32.66 | 100.11 | .893 |
| KR14 | 79°24.8′ | 30°24.2′ | 24.66 | .18 | 4.48 | 1.36 | .05 | 3.32 | 33.82 | .92 | .98 | .06 | 30.49 | 100.32 | .880 |
| KR15 | 79°24.8′ | 30°24.2′ | 46.88 | .37 | 9.38 | 2.10 | .06 | 4.66 | 15.68 | .74 | 2.64 | .08 | 17.37 | 99.95 | .708 |
| KR16 | 79°24.8′ | 30°24.2′ | 58.14 | .62 | 11.52 | 1.96 | .02 | 2.38 | 10.42 | .28 | 4.28 | .09 | 9.97 | 99.68 | .759 |
| Intercalated calc-silicates (Deoban Fm. ILHS): | | | | | | | | | | | | | | | |
| KR18 | 79°25.8′ | 30°26.8′ | 29.60 | .14 | 4.61 | 4.99 | .20 | 11.42 | 18.85 | .05 | 1.50 | .02 | 29.10 | 100.48 | .543 |
| KR83 | 79°23.81′ | 30°24.18′ | 58.55 | .30 | 7.18 | 2.80 | .07 | 2.92 | 13.18 | .68 | 1.48 | .11 | 12.69 | 99.96 | .765 |
| KR86 | 79°25.1′ | 30°24.5′ | 18.50 | .09 | 1.80 | 2.12 | .05 | 16.64 | 23.76 | .00 | .88 | .04 | 37.14 | 101.02 | .507 |
| KR88 | 79°25.77′ | 30°26.78′ | 33.30 | .22 | 3.95 | 1.87 | .08 | 5.00 | 26.35 | .49 | 1.17 | .03 | 27.35 | 99.81 | .791 |
| KR89 | 79°25.77′ | 30°26.78′ | 73.46 | .31 | 6.48 | 2.28 | .04 | 3.72 | 4.42 | .56 | 2.26 | .07 | 7.40 | 101.00 | .461 |
| KR92 | 79°25.75′ | 30°27.38′ | 40.67 | .29 | 7.47 | 2.29 | .04 | 11.76 | 12.91 | .04 | 3.01 | .07 | 21.26 | 99.81 | .441 |
| KR94 | 79°25.98′ | 30°27.88′ | 44.70 | .38 | 11.88 | 4.49 | .05 | 8.50 | 9.48 | .08 | 4.00 | .07 | 16.20 | 99.84 | .445 |
| KR95 | 79°25.98′ | 30°27.88′ | 33.29 | .24 | 6.07 | 4.64 | .08 | 10.93 | 16.41 | .07 | 2.13 | .04 | 26.02 | 99.91 | .519 |
| KR102 | 79°28.96′ | 30°29.17′ | 49.51 | .40 | 8.18 | 3.56 | .05 | 8.25 | 10.00 | .15 | 3.59 | .10 | 15.43 | 99.21 | .466 |
| Massive dolomite: | | | | | | | | | | | | | | | |
| Deoban Fm. ILHS: | | | | | | | | | | | | | | | |
| KR17 | 79°27.8′ | 30°28.3′ | 9.96 | .03 | .60 | .70 | .03 | 19.46 | 27.50 | .00 | .24 | .05 | 42.16 | 100.73 | .504 |
| KR68 | 78°59.85′ | 30°18.09′ | 2.20 | .01 | .04 | .52 | .04 | 21.20 | 29.88 | .00 | .00 | .01 | 45.92 | 99.83 | .504 |
| KR69 | 79°00.26′ | 30°18.00′ | 19.22 | .02 | .22 | 1.14 | .08 | 17.34 | 24.50 | .00 | .02 | .01 | 37.68 | 100.23 | .504 |
| KR90 | 79°25.71′ | 30°27.17′ | 9.36 | .06 | 1.02 | 1.16 | .04 | 19.28 | 27.32 | .00 | .34 | .02 | 42.14 | 100.72 | .505 |
| KR109 | 79°29.77′ | 30°31.19′ | 2.08 | .01 | .04 | .66 | .07 | 21.46 | 29.86 | .00 | .00 | .02 | 46.34 | 100.55 | .500 |
| OLHS: | | | | | | | | | | | | | | | |
| KR33 | 78°21.57′ | 30°07.50′ | 1.14 | .02 | .12 | .38 | .03 | 21.66 | 30.20 | .00 | .06 | .02 | 46.70 | 100.33 | .501 |
| KR34 | 78°21.57′ | 30°07.50′ | 5.08 | .02 | .28 | .76 | .09 | 20.82 | 29.04 | .00 | .10 | .05 | 44.90 | 101.15 | .501 |
| KR36 | 78°25.57′ | 30°06.98′ | .34 | .01 | .00 | .04 | .02 | 21.52 | 31.24 | .00 | .00 | .04 | 46.72 | 99.93 | .511 |

Note. Abbreviations: HHCS, High Himalayan Crystalline Series; ILHS, Inner Lesser Himalayan Series; OLHS, Outer Lesser Himalayan Series.

[a] Sample localities shown on figures 1 or 2. Grid references given to two decimal places are from GPS (WGS84), and one decimal place is taken from U.S. Army Corps of Engineers (1954).

[b] Loss on ignition.

[c] Ca/(Ca + Mg) molar ratio.

by two methods: (1) The carbonate fraction was dissolved in 10% glacial acetic acid for 10 min in an ultrasonic bath at room temperature and the solution separated from the residue by centrifuge. (2) A method suggested by Elderfield (pers. comm., 1998) was used that (*a*) was designed to remove easily exchangeable Sr and (*b*) was then followed by a leaching step that dissolved most of the calcite and dolomite. Exchangeable Sr was removed by adding 150 g of finely ground rock sample to 30 mL of 1 M ammonium chloride ($NH_4Cl$), pH 6.5. After 30 min in an ultrasonic bath, the mixture was then left overnight. After centrifuging, the supernatant fluid was filtered through 0.2 $\mu$m cellulose nitrate filters and the Sr separated. The residue was then treated with 3 mL of ammonium acetate buffer solution ($CH_3COONH_4$-$CH_3COOH$), pH 4.2, for 14 d at room temperature with 30 min in an ultrasonic

**Table 2.** Rb-Sr Isotopic Analyses of Whole Rock, Leaches, and Residues

| Sample | Distance (m) | East | North | Rb (ppm) | Sr (ppm) | Rb/Sr | $^{87}Sr/^{86}Sr$ wr | $^{87}Sr/^{86}Sr$ ac. leach | $^{87}Sr/^{86}Sr$ ac. res. |
|---|---|---|---|---|---|---|---|---|---|
| Badrinath traverse HHCS: | | | | | | | | | |
| KR25 | .00 | 79°29.37′ | 30°44.64′ | 31.35 | 59.65 | .5256 | .730237 | .723932 | |
| KR27 | 1.20 | 79°29.37′ | 30°44.64′ | 2.92 | 358.73 | .0081 | .710407 | | |
| KR28 | 1.55 | 79°29.37′ | 30°44.64′ | 6.27 | 312.50 | .0201 | .711488 | | |
| KR29 | 2.00 | 79°29.37′ | 30°44.64′ | 3.78 | 403.95 | .0094 | .710816 | .710819 | |
| KR30 | 2.35 | 79°29.37′ | 30°44.64′ | 2.20 | 451.33 | .0049 | .710397 | | |
| KR31 | 2.55 | 79°29.37′ | 30°44.64′ | 103.53 | 132.45 | .7817 | .732169 | | |
| 3.7 m carb band in schist: | | | | | | | | | |
| KR20 | | 79°29.84′ | 30°44.92′ | | | | | .722683 | |
| KR21 | | 79°29.84′ | 30°44.92′ | | | | | .715868 | |
| KR22 | | 79°29.84′ | 30°44.92′ | | | | | .751015 | |
| Traverse above Biri (Deoban Fm. ILHS): | | | | | | | | | |
| KR2 | .30 | 79°24.8′ | 30°24.2′ | 16.63 | 85.83 | .1938 | .739060 | | |
| KR3 | .95 | 79°24.8′ | 30°24.2′ | 21.62 | 76.78 | .2815 | .736825 | | |
| KR4 | 2.15 | 79°24.8′ | 30°24.2′ | 25.55 | 83.47 | .3061 | .741233 | | |
| KR5 | 3.00 | 79°24.8′ | 30°24.2′ | 40.73 | 72.87 | .5590 | .749696 | | |
| KR6 | 3.95 | 79°24.8′ | 30°24.2′ | 29.93 | 76.23 | .3927 | .752437 | | |
| KR7 | 4.75 | 79°24.8′ | 30°24.2′ | 27.63 | 79.88 | .3459 | .749991 | | |
| KR8 | 5.00 | 79°24.8′ | 30°24.2′ | 106.13 | 83.33 | 1.2653 | .775916 | | |
| KR9 | 5.90 | 79°24.8′ | 30°24.2′ | 82.53 | 58.53 | 1.4100 | .774609 | | |
| KR10 | 6.30 | 79°24.8′ | 30°24.2′ | 69.95 | 84.52 | .8277 | .772457 | | |
| KR11 | 6.62 | 79°24.8′ | 30°24.2′ | 33.42 | 71.63 | .4665 | .758061 | | |
| KR12 | 6.75 | 79°24.8′ | 30°24.2′ | 12.00 | 79.42 | .1511 | .724539 | | |
| KR13 | 6.90 | 79°24.8′ | 30°24.2′ | 30.90 | 80.12 | .3857 | .745946 | | |
| KR14 | 7.17 | 79°24.8′ | 30°24.2′ | 38.23 | 89.18 | .4287 | .758114 | | |
| KR15 | 7.22 | 79°24.8′ | 30°24.2′ | 100.42 | 55.82 | 1.7990 | .777420 | | |
| KR16 | 100.00 | 79°24.8′ | 30°24.2′ | 111.17 | 28.93 | 3.8422 | .802384 | | |
| Intercalated calc-silicate (Deoban Fm. ILHS): | | | | | | | | | |
| KR18 | | 79°25.8′ | 30°26.8′ | 71.12 | 91.32 | .7788 | 1.184132 | 1.188086 | 1.182208 |
| KR19 | | 79°25.8′ | 30°26.8′ | 1110.77 | 7.09 | 156.67 | 1.310834 | 1.071700 | |
| KR83 | | 79°23.81′ | 30°24.18′ | 62.75 | 69.68 | .9005 | .799089 | .798674 | .801428 |
| KR86 | | 79°25.1′ | 30°24.5′ | 29.28 | 42.48 | .6893 | .887962 | .884691 | |
| KR88 | | 79°25.77′ | 30°26.78′ | 46.53 | 100.20 | .4644 | .870568 | .868826 | |
| KR92 | | 79°25.75′ | 30°27.38′ | 111.12 | 34.63 | 3.2088 | .897470 | .886241 | .905639 |
| KR94 | | 79°25.98′ | 30°27.88′ | 156.53 | 30.43 | 5.1439 | 1.085612 | 1.068025 | 1.097645 |
| KR95 | | 79°25.98′ | 30°27.88′ | 85.87 | 47.32 | 1.8147 | 1.039948 | | |
| KR102 | | 79°28.96′ | 30°29.17′ | 104.28 | 31.45 | 3.3157 | .930854 | | |
| Massive dolomite: | | | | | | | | | |
| ILHS: | | | | | | | | | |
| KR17 | | 79°27.8′ | 30°28.3′ | 7.20 | 22.63 | .3182 | .735385 | .734415 | .735622 |
| KR69 | | 79°00.26′ | 30°18.00′ | .01 | 26.73 | .0004 | .710100 | .711343 | |
| KR109 | | 79°29.77′ | 30°31.19′ | .00 | 51.92 | .0000 | .716064 | .715858 | |
| OLHS: | | | | | | | | | |
| KR34 | | 78°21.57′ | 30°07.50′ | 2.72 | 88.63 | .0307 | .713421 | | |
| KR36 | | 78°28.57′ | 30°06.98′ | .00 | 37.45 | .0000 | .709816 | | |

Note. Abbreviations: wr, whole rock; ac., acetic acid; res., residue. For additional abbreviations, see table 1.

bath each day. The supernatant fluid was then centrifuged and filtered as above. Experiments using synthetic mixtures of Himalayan silicate gneisses and natural carbonate and dolomites (Bunbury et al. 2000) showed that the ammonium chloride stage removed ~5% of Sr from silicate samples and ~20% of Sr from carbonate samples (both calcite or dolomite) and that total recovery of Sr from the carbonate fractions was ~85%.

## Carbonates and Calc-Silicates from the High Himalayan Crystalline Series

Carbonate rocks form only a small part of the High Himalayan Crystalline Series. Le Fort (1975) describes carbonates in some sections of the High Himalayan Crystalline Series in Nepal (Formation 2). Further east, in the Langtang and Nyalam sections, carbonates are almost entirely absent (Inger and Harris 1992; Hodges et al. 1993). In the Garhwal Himalaya, the High Himalayan Crystalline Series, locally known as the Vaikrita Group, is dominated by high-grade schists and gneisses, but an ~1-km-thick unit of intercalated silicates and carbonates has been mapped west of Badrinath near the Saraswati River, a major tributary of the Alaknanda (e.g., KR25-31 on fig. 1), and a number of thin carbonate and calc-silicate horizons have been described (e.g., samples KR20-22 on fig. 1; Misra and

**Table 3.** Rb-Sr Isotopic Compositions of Multiple Leaches

| | Badrinath traverse/ KR26 | Biri traverse ILHS/KR1 | Intercalated calc-silicate ILHS/KR89 | Massive dolomite | | |
|---|---|---|---|---|---|---|
| | | | | ILHS | | OLHS |
| | | | | KR68 | KR90 | KR33 |
| Distance[a] | .95 | −.75 | | | | |
| East | 79°29.37′ | 79°24.8′ | 79°25.77′ | 78°59.85′ | 79°25.71′ | 78°21.57′ |
| North | 30°44.64′ | 30°24.2′ | 30°26.78′ | 30°18.09′ | 30°27.17′ | 30°07.50′ |
| Rb (ppm) | 48.53 | 73.5 | 100.05 | .01 | 8.6 | 1.02 |
| Sr (ppm) | 48.4 | 111.8 | 28.87 | 30.38 | 23.1 | 93.13 |
| Rb/Sr | 1.0028 | .6574 | 3.4655 | .0003 | .3723 | .0110 |
| $^{87}Sr/^{86}Sr$: | | | | | | |
| Whole rock | .716067 | .772586 | 1.061393 | .708760 | .734177 | .713202 |
| Acetic acid leach | | .711150 | 1.050503 | .710439 | .728473 | .713177 |
| Acetic acid residue | | .778102 | | | | |
| Exchangeable leach: | | | | | | |
| $^{87}Sr/^{86}Sr$ | .715373 | .769639 | 1.009880 | .713211 | .727340 | .713445 |
| Sr (%) | 11.7 | 19.6 | 12.7 | 8.6 | 6.8 | 6.5 |
| $^{87}Rb/^{86}Sr$ | .3249 | .0964 | .7768 | .0319 | .2470 | .0268 |
| Ammonium leach: | | | | | | |
| $^{87}Sr/^{86}Sr$ | .715347 | .770893 | 1.045362 | .708625 | .725934 | .712884 |
| Sr (%) | 5.3 | 55.2 | 60.1 | 60.3 | 51.3 | 54.7 |
| $^{87}Rb/^{86}Sr$ | .7818 | .0332 | .1544 | .0080 | .0436 | .0041 |
| Ammonium residue: | | | | | | |
| $^{87}Sr/^{86}Sr$ | .716813 | .787421 | 1.116143 | .706780 | .790472 | .725534 |
| Sr (%) | 63.6 | 10.2 | 14.0 | 8.3 | 8.1 | 1.3 |
| $^{87}Rb/^{86}Sr$ | 3.2601 | 14.3888 | 56.0524 | .0197 | 8.7576 | 1.2571 |

[a] Distances on traverses (other samples in table 2).

Sharma 1973; Gairola 1975). To the west, in the Bhagirathi Valley, Metcalfe (1990) maps a total of ~2 km of calc-silicates within the ~25-km-thick Munsiari and Vakrita Crystalline Formations.

The Badrinath traverse was sampled from the ~1-km-thick unit of calc-silicates exposed southwest of Badrinath (fig. 1). The traverse comprises intercalations of quartzites, calc-silicates, and impure metalimestones exposed over a distance of 10 m and sampled in detail over 2.5 m (fig. 4). The calc-silicates are medium-grained assemblages of calcite, diopside, amphibole, quartz, plagioclase, and phlogopite with amphibole typically replacing the diopside. For the limestones (>80% carbonate), Sr values (350–450 ppm) are only slightly lower than typical marine values (500–600 ppm). The calc-silicate horizons have lower Sr (50–300 ppm) than the carbonate-rich horizons. The moderate $^{87}Sr/^{86}Sr$ ratios (~0.711) of the more pure carbonate lithologies are unsupported in that their Rb/Sr ratios are too low to generate the $^{87}Sr/^{86}Sr$ ratios for plausible initial $^{87}Sr/^{86}Sr$ ratios. For example, assuming the maximum age of 1800 Ma and Rb/Sr = 0.02 results in a $^{87}Sr/^{86}Sr$ ratio of 0.7105 from a high initial $^{87}Sr/^{86}Sr$ ratio of 0.709 (marine $^{87}Sr/^{86}Sr$ ratios were probably ~0.705 at 1800 Ma; Veizer 1989). However, these ratios could be obtained from isotopic exchange between silicate and carbonate lithologies. For example, mass balance calculation indicates that the $^{87}Sr/^{86}Sr$ ratio of 0.71082 for KR29 (Sr = 404 ppm) could result from the exchange of 0.5% of the Sr from the schist KR25 (Sr = 60 ppm, $^{87}Sr/^{86}Sr$ = 0.72393) if the carbonate had an initial

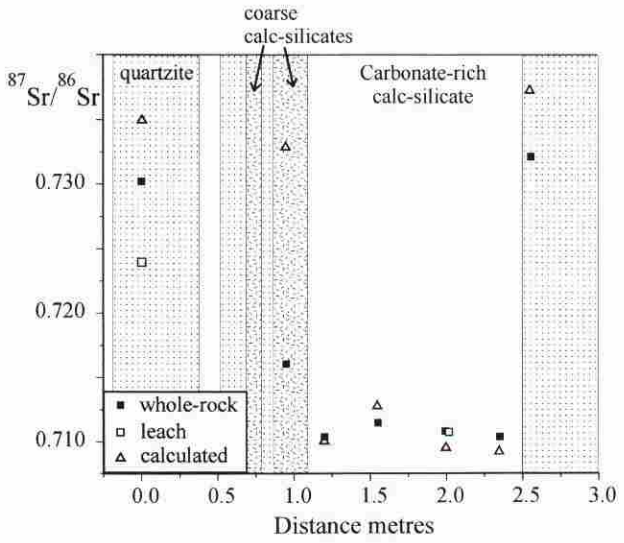


**Figure 4.** Sr isotopic profile of calc-silicate and carbonate traverse near Badrinath. Leaches are one-stage acetic acid. Quartzite contains calc-silicate minerals. Calculated $^{87}Sr/^{86}Sr$ ratios are based on estimated initial Sr isotopic composition and age (see text).

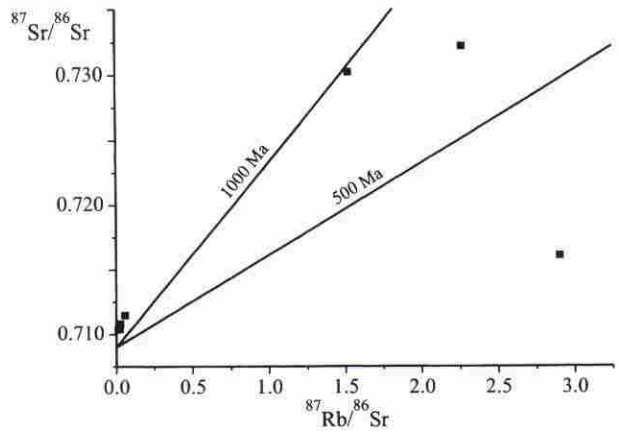


**Figure 5.** Whole-rock samples from Badrinath traverse plotted on isochron diagram; 500- and 1000-Ma lines for initial $^{87}Sr/^{86}Sr = 0.709$ are shown for reference.

$^{87}Sr/^{86}Sr = 0.709$ at 500 Ma. However, the bulk rock samples from the traverse do not define an isochron (fig. 5) precluding an event that completely homogenized Sr isotopic compositions on an ~3-m-length scale.

The relative shifts in isotopic composition along the profile are consistent with exchange of Sr. The original Sr isotopic compositions of the carbonate and silicate fractions are not known, but it is possible to make rough estimates of their compositions to compare the relative compositions of the low Rb/Sr carbonate and high Rb/Sr silicate layers. Figure 4 shows Sr isotopic compositions calculated assuming that (1) a pelitic end-member had a $^{87}Sr/^{86}Sr$ ratio of 0.725 at 500 Ma, (2) a carbonate end-member had a $^{87}Sr/^{86}Sr$ ratio of 0.708 at 500 Ma, and (3) the original (500 Ma) fraction of carbonate in each sample ($C_b$) before any decarbonation reactions is given by

$$C_b = \frac{CaO + 1.4MgO}{56}, \quad (1)$$

where CaO and MgO are oxides in weight percent. The calculation assumes that all the CaO and MgO derive from carbonate, and thus equation (1) gives a maximum limit to the carbonate fraction. The results show that the pelitic, high $^{87}Sr/^{86}Sr$ samples have lost $^{87}Sr$ and the low $^{87}Sr/^{86}Sr$ samples gained $^{87}Sr$, with the largest changes across the highest gradients in $^{87}Sr/^{86}Sr$ ratios (e.g., across the carbonate contact at ~1.2 m). An alternative explanation, that the carbonate-rich rocks have lost Rb and the more pelite-rich rocks gained Rb, is less likely because the carbonate-rich rocks are likely to have originally contained less Rb and the decarbonation reactions are likely to create new Rb-bearing phases such as amphibole in the siliceous dolomite rocks.

The timing of the exchange is not well constrained because the High Himalayan Crystalline Series rocks have undergone multiple metamorphic events. Mineral separates, leaches, and residues of sample KR26 (tables 2–4) scatter about a 15.0 ± 1.5 Ma ($2\sigma$) regression line on an isochron diagram (fig. 6) where the age is controlled by the high Rb/Sr biotite separate. This biotite age is within the range of K-Ar muscovite and biotite ages obtained by Metcalfe (1993) on the Garhwal High Himalayan Crystalline Series. The scatter of the amphibole, pyroxene, carbonate (leached), and residue from leaching about the regression are interpreted to result from the variable closure temperatures of the minerals and the complex mineralogical evolution of the sample. However, despite the best estimate of the isotopic composition of the carbonate fraction from the ammonium acetate leach not being in isotopic equilibrium with the whole-rock, biotite, and feldspar fractions at 15 Ma, a regression line through this leach composition, whole rock,

**Table 4.** Rb-Sr Isotopic Analyses of Mineral Separates

| Sample | Mineral separates | Rb | Sr | Rb/Sr | $^{87}Rb/^{86}Sr$ | $^{87}Sr/^{86}Sr$ | $1\sigma$ |
|---|---|---|---|---|---|---|---|
| KR89C | Leach | .12 | .13 | .93 | 2.78 | 1.046031 | 11 |
| KR89F | Feldspar 1 | 2.51 | .28 | 9.04 | 27.15 | 1.092266 | 20 |
| KR89F2 | Feldspar 2 | 68.33 | 4.98 | 13.72 | 41.23 | 1.104808 | 7 |
| KR89PA[a] | Phlogopite | 176.64 | 7.29 | 24.24 | 73.31 | 1.171664 | 6 |
| KR89PB[a] | Phlogopite | 223.59 | 7.5 | 29.80 | 71.81 | 1.192905 | 1913 |
| KR89PC[a] | Muscovite-phlogopite | 132.22 | 7.28 | 18.15 | 54.92 | 1.174853 | 6 |
| KR89PD[a] | Muscovite | 102.38 | 18.83 | 5.44 | 16.23 | 1.032825 | 27 |
| KR26A | Amphibole | 14.12 | 6.09 | 2.32 | 6.72 | .716637 | 21 |
| KR26B | Biotite | 858.49 | 2.65 | 323.74 | 956.45 | .923477 | 61 |
| KR26F | Feldspar 1 | 1.68 | 16.21 | .10 | .30 | .715686 | 7 |
| KR26F1 | Feldspar 2 | 56.04 | 278 | .20 | .58 | .715709 | 7 |
| KR26P | Pyroxene | 4.56 | 8.75 | .52 | 1.51 | .716454 | 119 |

[a] Mixed phlogopite-muscovite separates with A, most phlogopite rich, to D, most muscovite rich.

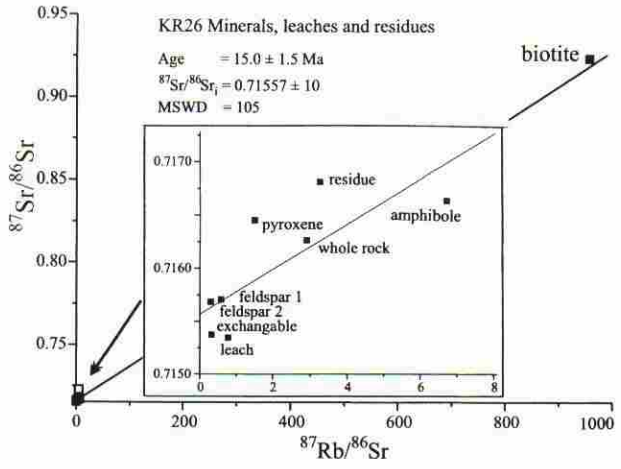


**Figure 6.** Isochron diagram for whole rock, mineral separates, and leach of exchangeable Sr, carbonate, and residue from leaching sample KR26 from High Himalayan Crystalline Series calc-silicate from near Badrinath (table 2). Open square is acetic acid leach not included in regression. Note that age depends on the biotite fraction.

and the residue gives an age of 31 ± 6 Ma (initial $^{87}Sr/^{86}Sr = 0.71500 \pm 17$ [$2\sigma$], MSWD = 6.3). As expected, carbonate in these high-grade rocks came to equilibrium with the silicate fraction during the Himalayan metamorphism.

## Carbonates and Calc-Silicates from the Inner Lesser Himalaya

Carbonates from the Inner Lesser Himalaya are potentially important for this study since some studies of Himalayan riverine chemistry find that the dissolved $^{87}Sr/^{86}Sr$ of surface waters increases most dramatically while flowing across this section of the Himalaya (Derry and France-Lanord 1996; Harris et al. 1998; English et al. 2000), although other authors find that the contribution of Lesser Himalayan carbonates to the river fluxes is small (e.g., Krishnaswami and Singh 1998; Singh et al. 1998; Galy et al. 1999; Krishnaswami et al. 1999). The most extensive carbonate lithologies exposed in the Lesser Himalaya of Garwhal occur within the Deoban Formation. This unit comprises cherty dolomites, dolomitic limestones with intercalations of slate, limestones and dolomites associated with stromatolitic bioherms, as well as a range of calc-silicates containing variable fractions of calcite, dolomite, quartz, plagioclase, chlorite, muscovite, and phlogopite (Gairola 1975; Kumar and Tewari 1978; Valdiya 1995).

We have sampled the range of massive dolomites, limestones, and calc-silicates representative of the Alaknanda section through the Deoban Formation, together with a detailed traverse of contrasting carbonate and silicate lithologies at Biri (fig. 2). Analyses of whole-rock samples, acetic acid leaches, and residues from leaching (tables 1–3) and analyses from Singh et al. (1998) are illustrated on a plot of $^{87}Sr/^{86}Sr$ versus Ca/(Ca + Mg) molar fraction in figure 7 and on an isochron plot in figure 8. Figure 7 shows that extreme $^{87}Sr/^{86}Sr$ values occur only in dolomitic calc-silicate samples, although both the more pure dolomites and limestones have elevated $^{87}Sr/^{86}Sr$ ratios that range up to 0.75.

Nearly all the carbonate samples from the Deoban Formation have high whole-rock $^{87}Sr/^{86}Sr$ ratios. Massive dolomites and limestones have $^{87}Sr/^{86}Sr$ ratios between 0.708 and 0.750 and values greater than 1.0 in calc-silicates (fig. 8). Acetic acid leaches give $^{87}Sr/^{86}Sr$ ratios close to whole-rock values, confirming that the carbonate fraction shares the high $^{87}Sr/^{86}Sr$ ratios (fig. 8). In two samples (KR18 and KR69), the leach $^{87}Sr/^{86}Sr$ ratio exceeds that of the whole rock, and we suspect that the acetic acid leaching released some exchangeable Sr from the silicate in addition to Sr from the carbonate. This is confirmed by the ammonium chloride leaches of samples KR68, KR90, and KR89 in which the exchangeable Sr leach is more radiogenic than the whole-rock Sr, whereas the subsequent ammonium acetate leach (the carbonate fraction) is less radiogenic (fig. 8; table 3), although this does not hold for sample KR1.

On an isochron plot (fig. 8), the Sr isotope ratios of most calc-silicate samples lie on or below the 2500-Ma reference line with an initial $^{87}Sr/^{86}Sr$

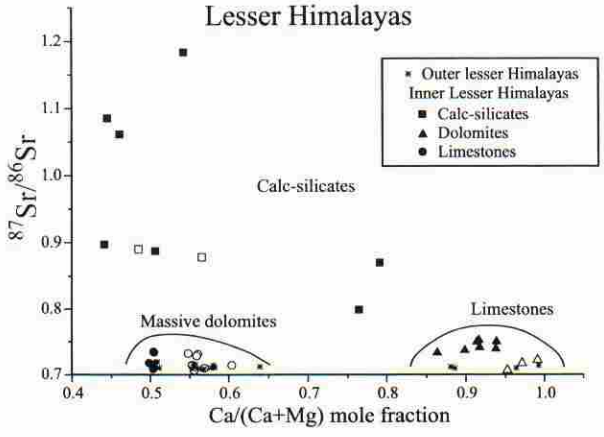


**Figure 7.** $^{87}Sr/^{86}Sr$ versus CaO to CaO + MgO molar ratio for Inner Lesser Himalayan samples (*open symbols*, Singh et al. 1998; *filled symbols*, this study).

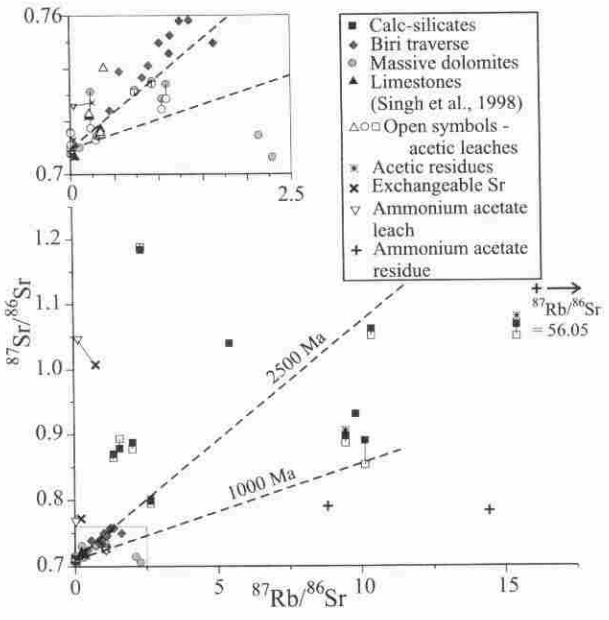


**Figure 8.** Isochron plot of carbonate samples from the Inner Lesser Himalayas. Acetic acid leaches and residues plotted with Rb/Sr ratios of whole-rock samples. Note that $^{87}Sr/^{86}Sr$ ratios of many samples are supported by their $^{87}Rb/^{86}Sr$ ratios if their depositional age is ~2500 Ma. Acetic acid leaches with no measurement of Rb/Sr ratios are joined to whole-rock values and plotted at the whole-rock $^{87}Rb/^{86}Sr$ values.

ratio = 0.710. The $^{87}Sr/^{86}Sr$ ratios in these samples are supported by their $^{87}Sr/^{86}Sr$ ratios within a Proterozoic time span. At least some of the unsupported samples may have exchanged Sr with adjacent Rb-rich shales by diffusive or advective processes involving the fluid phase. For example, carbonate sample KR18 ($^{87}Sr/^{86}Sr$ ratio = 1.184) was collected adjacent to a contact with shale, and the adjacent high Rb/Sr shale sample, KR19, has a $^{87}Sr/^{86}Sr$ ratio of 1.31. The magnitude and scale length of Sr isotopic exchange in Lesser Himalayan Formations has been investigated at the Biri locality discussed below.

***The Biri Traverse.*** A more detailed study of intercalated calc-silicates has been undertaken in the Biri traverse, an 8-m-long section that encompasses impure limestones and calc-silicates of varying carbonate/silicate proportions from the Deoban Formation. Figure 9 illustrates how the variation of Rb/Sr mirrors that of $Al_2O_3$, a measure of the pelite fraction in the rock. $^{87}Sr/^{86}Sr$ ratios vary from 0.733 in the carbonate-rich samples to 0.775 in the more pelitic samples. The calc-silicate assemblages include dolomite, quartz, plagioclase, chlorite, and muscovite with graphite, sphene, and tourmaline as accessory minerals. As for the Badrinath traverse, Rb/Sr and the silicate content of the bulk rock correlates closely with $^{87}Sr/^{86}Sr$, and the heterogeneities in $^{87}Sr/^{86}Sr$ are preserved on length scales greater than ~0.5 m. On an isochron diagram (fig. 10), the samples scatter widely about an ~450-Ma regression line. Pelite-rich samples (KR1, KR8, KR9, KR10, and KR15) lie close to an ~118-Ma reference line. However, these regressions may reflect mixing, and their age significance is dubious.

The Sr isotopic profile at Biri is shown in figure 11. Quantitative interpretation of such profiles requires good estimates of both the initial state and timing of Rb-Sr isotopic mobility (e.g., Bickle et al. 1997), but it is possible to evaluate the extent and direction of Sr isotopic or Rb/Sr mobility by comparison of the observed $^{87}Sr/^{86}Sr$ profile with a "model" profile calculated on the basis of estimated ages and initial $^{87}Sr/^{86}Sr$ ratios. The model profile is calculated to simulate the present-day profile in the absence of diffusive or advective transport of Sr. This is done by estimating the initial $^{87}Sr/^{86}Sr$ ratio of the rocks, estimating the age at which they had this initial ratio, and presuming that the whole-rock Rb/Sr ratios have remained unchanged. The model profile shown in figure 11 assumes that both carbonate and silicate rocks had an initial $^{87}Sr/^{86}Sr$ ratio of 0.702 at 1300 Ma. Comparison of the measured $^{87}Sr/^{86}Sr$ ratios with the model values shows that most pelite-rich samples have lower $^{87}Sr/^{86}Sr$ ratios and carbonate-rich samples have higher $^{87}Sr/^{86}Sr$ ratios than the model calculations (fig. 11). Assumption of a lower initial $^{87}Sr/^{86}Sr$ ratio for the carbonate fraction than for the

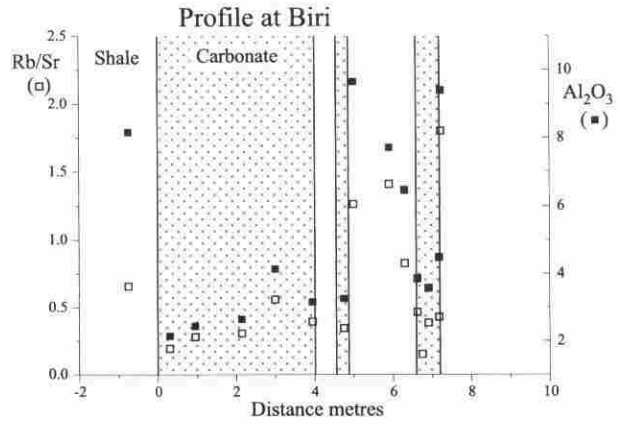


**Figure 9.** Rb/Sr and $Al_2O_3$ (wt %) across Biri profile showing contrast between shale- and carbonate-rich lithologies. Lithological boundaries are as identified in field.

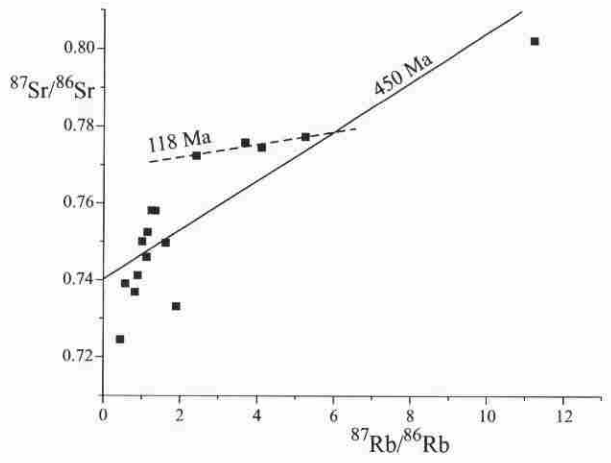


**Figure 10.** Samples from Biri traverse (including KR16 collected ~100 m north of profile) plotted on an isochron diagram. Regression lines of 450 Ma (all data) and ~118 Ma (pelite-rich samples KR1, 8, 9, 10, and 15) probably have limited or no age significance.

pelite fraction would accentuate this difference, and assumption of younger or older ages, while changing the discrepancy between the measured and model values, does not alter the conclusion that the carbonate rocks have gained $^{87}Sr$ at the expense of the more radiogenic pelitic samples. The more marked shifts between observed and model $^{87}Sr/^{86}Sr$ ratios on both margins of the carbonate horizons (e.g., KR2 and KR6 vs. KR3, KR4, and KR5; KR11 and KR14 vs. KR10 and KR15) implies that Sr isotopic diffusive transport distances were on the order of 10–30 cm within the range observed in other metamorphic terrains (Bickle et al. 1995, 1997). Asymmetry in the profile resulting from advective transport is not resolved at length scales greater than the ~20-cm resolution of the data.

The timing of the exchange is not well constrained except that the magnitude of the shifts requires several hundred millions of years to have elapsed (or any early diagenetic isotopic homogenization) to allow Sr isotopic heterogeneities to develop before the partial isotopic homogenization observed. A regression line though the pelitic samples gives a very poorly constrained age of 118 ± 51 Ma (fig. 10). Plagioclase, muscovite, and phlogopite fractions were separated from sample KR89, as well as leaching carbonate (tables 2–4). The muscovite is crenulated by a prominent fabric possibly related to movement on the nearby MCT, and the phlogopite grows across this fabric, possibly related to Himalayan metamorphism. However, complete separation of phlogopite and muscovite was not possible, and the phlogopite-rich fractions (KR89PA, PB, PC, and PD) contain 20%–50% phlogopite. The minerals (including two feldspar fractions and the whole-rock ammonium acetate leach and residue but excluding two of the phlogopite fractions [PC and PD] and the exchangeable Sr fraction) give a regression line corresponding to an age of 110 ± 26 Ma ($2\sigma$) (fig. 12). This is similar to the regression through the Rb-Sr isotopic compositions of the pelitic rocks from the Biri traverse but of uncertain geological significance. The age may be dominated by the older muscovite fraction.

***Massive Dolomites.*** The great majority of massive carbonates in the Inner Lesser Himalayas are dolomites. All such samples have unusually low Sr (20–50 ppm) and moderate $^{87}Sr/^{86}Sr$ (0.710–0.735) (see fig. 13), similar to values documented by Singh et al. (1998) from Garhwal dolomites exposed farther west (Sr = 20–70 ppm; $^{87}Sr/^{86}Sr$ = 0.706–0.732). All massive dolomites are supported over 2500 Ma; for example the $^{87}Sr/^{86}Sr$ of 0.735 for KR17 can be obtained internally in 1600 Ma. All the massive dolomites in the Inner Lesser Himalayas are characterized by high Ca/Sr ratios (Ca/[1000 Sr] molar ratio = 10–20), providing a possible source for high Ca/Sr fluids without recourse to vein calcite as invoked for the elevation of $^{87}Sr/^{86}Sr$ in carbonates from the western Himalaya (Blum et al. 1998).

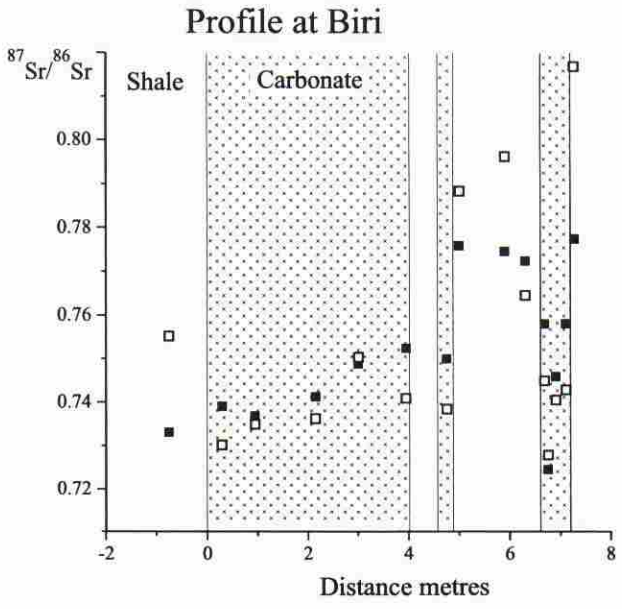


**Figure 11.** Profile across intercalated carbonate-bearing shales and impure limestones near Biri (fig. 3). Solid symbols are present-day $^{87}Sr/^{86}Sr$ ratios; open symbols are model $^{87}Sr/^{86}Sr$ ratios, calculated assuming the initial $^{87}Sr/^{86}Sr$ = 0.720 at 1300 Ma.

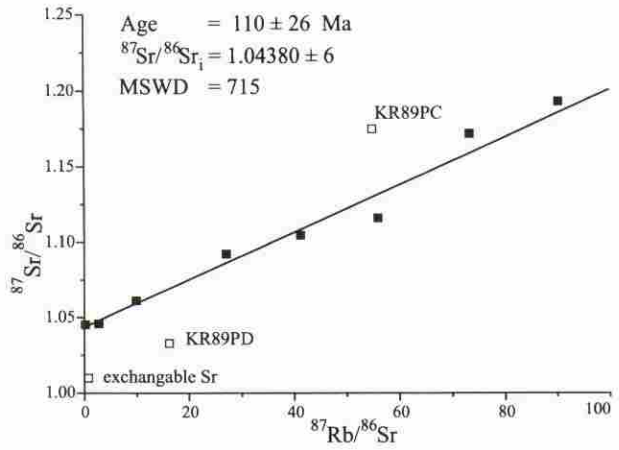


**Figure 12.** Regression line through mineral separates and whole-rock composition from KR89. Exchangeable Sr and two of the four phlogopite separates (*PC* and *PD*) have not been included in regression.

### Carbonates from the Outer Lesser Himalaya

The dominant carbonate lithologies from the Outer Lesser Himalaya occur within the Krol Formation, comprising limestones, slates, and siltstones overlain by massive dolomites. Their deposition age has been ascribed to the uppermost Proterozoic (Valdiya 1995).

The massive dolomites of the Krol Formation are characterized by low Sr (37–93 ppm) and very low Rb abundances. The massive dolomites from the Outer Lesser Himalayas have somewhat lower $^{87}Sr/^{86}Sr$ ratios (0.709–0.715) compared with dolomites from the Inner Lesser Himalayas (0.71–0.75) (fig. 8). $^{87}Sr/^{86}Sr$ ratios in most of the carbonates from the Outer Lesser Himalayas are mostly supported, given an initial $^{87}Sr/^{86}Sr$ ratio of 0.710 and an age of 2500 Ma (fig. 13). Massive limestones from the Outer Lesser Himalayas (Singh et al. 1998) have slightly lower Sr isotope ratios (giving an average $^{87}Sr/^{86}Sr$ of 0.7104) compared with that for dolomites (0.7116), which is partly explained by their lower Rb/Sr ratios (0.001 compared with 0.038). However, the spread in $^{87}Sr/^{86}Sr$ ratios from 0.709 to 0.714 for limestones and dolomites from the Outer Lesser Himalayas with very low Rb/Sr ratios (fig. 13) is evidence for diagenetic or later Sr isotopic mobility associated with dolomitization or metamorphic diffusive or advective transport of $^{87}Sr$ from adjacent silicate lithologies. Acetic acid leaches of two dolomite samples give $^{87}Sr/^{86}Sr$ ratios of the carbonate fraction close to whole rock, and the ammonium acetate leach and residue from sample KR33 gives a Rb-Sr age of ~700 Ma. In contrast, leaches of the limestones by Singh et al. (1998) give relatively low $^{87}Sr/^{86}Sr$ ratios between 0.7085 and 0.7097 and impossibly large minimum leach whole-rock ages, indicating the carbonate was never in equilibrium with the silicate fraction.

### Impact on Riverine $^{87}Sr/^{86}Sr$ Ratios

This geochemical study of carbonate lithologies from the Garhwal Himalaya has established that within the High Himalayan Crystalline Series, $^{87}Sr/^{86}Sr$ ratios of carbonates are raised to values from 0.710 in pure carbonates to 0.724 in calc-silicates. This compares with $^{87}Sr/^{86}Sr$ ratios of 0.714–0.718 in the High Himalayan Crystalline Series in Nepal (Galy et al. 1999), ~0.724 in leaches from the bed load of the Bhote Kosi River where it transgresses the High Himalayan Crystalline Series in Nepal (Harris et al. 1998), and 0.715 in a leach of bed load from a tributary to the Seti River in the High Himalayan Crystalline Series in Western Nepal (English et al. 2000). In the Inner Lesser Himalayas, the results of this study and that of Singh et al. (1998) show that carbonate $^{87}Sr/^{86}Sr$ ratios range up to 0.735 in pure dolomites, to 0.750 in calcitic calc-silicates, and as high as 1.200 in dolomitic calc-silicates. In Nepal, Galy et al. (1999) record values for carbonates of 0.717–0.857 in the Lesser Hima-

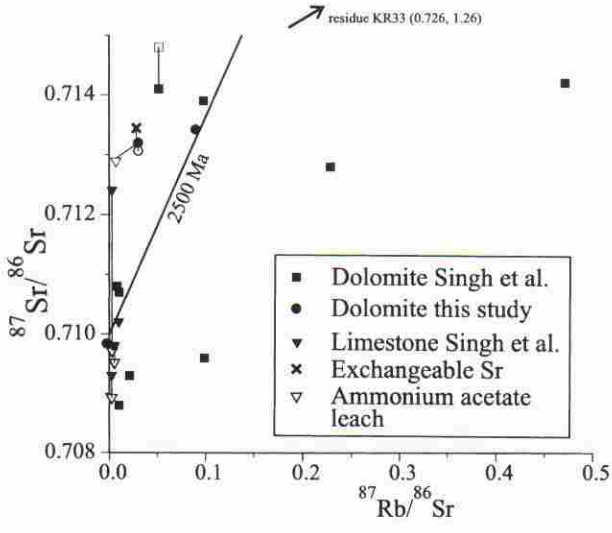


**Figure 13.** Isochron diagram for samples from Outer Lesser Himalayas. Data from Singh et al. (1998) and this study. Acetic acid leaches attached to corresponding whole-rock $^{87}Sr/^{86}Sr$ ratio by line and plotted at same $^{87}Rb/^{86}Sr$ ratio. Exchangeable Sr and ammonium acetate leach from KR33 are shown; residue has $^{87}Sr/^{86}Sr$ = 0.7255; $^{87}Rb/^{86}Sr$ = 1.257.

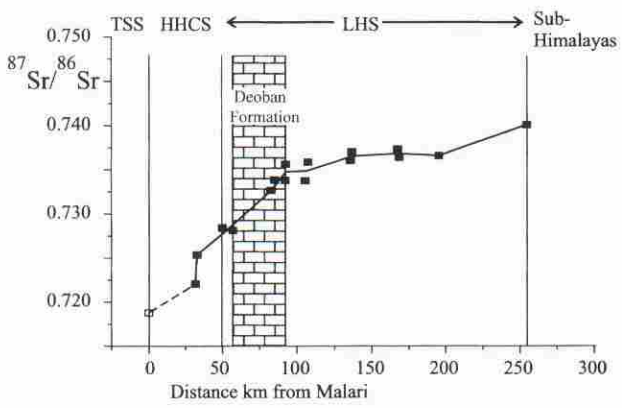


**Figure 14.** Sr isotopic profiles of water samples down the Alaknanda in September 1998, except sample at Malari on South Tibetan Detachment Zone collected in October 1997. Distance is in kilometers downstream from Malari on the South Tibetan Detachment Zone. The Munsiari Thrust is 50 km downstream, and the Himalayan Frontal Thrust is about 255 km downstream.

layas. These values compare with a $^{87}Sr/^{86}Sr$ ratio of 0.791 on the leach fraction from the bed load of the Bhote Kosi River within the Lesser Himalayan Series in Nepal (Harris et al. 1998) and between 0.730 and 1.003 for leaches of carbonate detritus in tributaries to the Seti River draining the Lesser Himalayan Series in western Nepal (English et al. 2000). Carbonates from the Outer Lesser Himalayas have $^{87}Sr/^{86}Sr$ ratios up to, but not exceeding, 0.715 (this study and results of Singh et al. 1998).

Extreme $^{87}Sr/^{86}Sr$ ratios (0.8–1.2) obtained in this study are therefore peculiar to the dolomitic calc-silicate intercalations from the Deoban Formation, exposed in the Alaknanda section between Helang and Nandapryag. The riverine $^{87}Sr/^{86}Sr$ of the Alaknanda mainstream increases particularly rapidly over this section (from ~0.728 to 0.735 in September 1998; fig. 14). Tributaries draining the calc-silicates carry dissolved values of $^{87}Sr/^{86}Sr$ ranging from 0.753 to 1.240 (table 5), and the correspondence between these values and those of the carbonate fractions of the rock samples indicates that the carbonates contribute a significant fraction of the high $^{87}Sr/^{86}Sr$ ratios in this section. The results of quantitative modeling of $^{87}Sr$ inputs into the Alaknanda River will be presented in a separate article and confirm that carbonate rocks in the Lesser Himalayan Series make a significant, but not dominant, contribution to the $^{87}Sr$ budget of the Alaknanda River.

In a recent compilation of Sr data for Himalayan carbonates (Singh et al. 1998), only two are characterized by strongly elevated $^{87}Sr/^{86}Sr$ ratios (>0.87), both of which are dolomitic calc-silicates rather than pure carbonates. Singh et al. (1998, p. 754) invoke the apparent rarity of carbonates with such high ratios and the relatively high Sr/Ca ratios of the river waters to conclude that "on a basin wide scale the carbonates are unlikely to be a major contributor to the high $^{87}Sr/^{86}Sr$ ratios in the source waters," although they recognize that high $^{87}Sr/^{86}Sr$ ratio carbonates may dominate particular streams. This presupposes that weathering results in congruent dissolution, but even if this is the case, our study indicates that very high dissolved Sr isotope ratios may be derived from carbonate weathering from calc-silicate lithologies within the Inner Lesser Himalayas and that input of Sr from the Deoban Formation is characterized by $^{87}Sr/^{86}Sr$ ratios of 0.8 or more.

Galy et al. (1999) conclude that Lesser Himalayan carbonates make a minor contribution to the Sr

**Table 5.** $^{87}Sr/^{86}Sr$ Ratios of Water Samples Collected September 1998

| Sample | $^{87}Sr/^{86}Sr$ | 1σ | North[a] | East |
|---|---|---|---|---|
| AK121 | .740063 | 16 | 30°7.35′ | 78°18.66′ |
| AK122 | .744473 | 16 | 30°8.42′ | 78°35.77′ |
| AK123 | .735683 | 8 | 30°8.74′ | 78°35.86′ |
| AK125 | .739602 | 7 | 30°13.00′ | 78°44.33′ |
| AK126 | .737318 | 8 | 30°13.49′ | 78°46.40′ |
| AK127 | .728095 | 8 | 30°31.58′ | 79°30.02′ |
| AK129 | .734670 | 7 | 30°19.93′ | 79°19.09′ |
| AK130 | .736311 | 7 | 30°19.87′ | 79°18.58′ |
| AK133 | .735364 | 8 | 30°15.75′ | 79°12.96′ |
| AK134 | .737118 | 7 | 30°15.96′ | 79°12.06′ |
| AK136 | .737111 | 41 | 30°17.30′ | 78°58.70′ |
| AK137 | .732879 | 25 | 30°19.93′ | 79°19.09′ |
| AK139 | .733814 | 6 | 30°24.03′ | 79°19.77′ |
| AK142 | .725901 | 7 | 30°93.75′ | 79°34.56′ |
| AK144 | .728391 | 5 | 30°34.30′ | 79°33.14′ |
| AK146 | .722041 | 5 | 30°29.27′ | 79°41.44′ |
| AK147 | .725355 | 5 | 30°29.25′ | 79°40.85′ |
| AK150 | .732645 | 5 | 30°24.03′ | 79°19.77′ |
| AK152 | .732863 | 7 | 30°19.93′ | 79°19.09′ |
| AK154 | .734933 | 10 | 30°19.87′ | 79°18.58′ |
| AK157 | .732084 | 10 | 30°15.75′ | 79°12.96′ |
| AK158 | .734576 | 32 | 30°15.96′ | 79°12.06′ |
| AK161 | .736996 | 7 | 30°17.13′ | 78°58.45′ |
| AK163 | .734912 | 8 | 30°17.30′ | 78°58.70′ |
| AK165 | .736405 | 8 | 30°12.81′ | 78°45.79′ |
| AK169 | .737442 | 8 | 30°8.74′ | 78°35.86′ |
| AK109[b] | .718733 | 9 | 30°33.67′ | 79°47.71′ |
| AK79[b,c] | .903728 | 16 | 30°27.66′ | 79°26.68′ |
| AK80[b,c] | 1.243866 | 13 | 30°27.92′ | 79°27.45′ |
| AK81[b,c] | .753147 | 14 | 30°29.24′ | 79°29.18′ |
| AK140[c] | .913099 | 9 | 30°24.96′ | 79°25.90′ |
| AK141[c] | .771971 | 22 | 30°24.41′ | 79°23.42′ |

[a] Localities shown on figure 1.
[b] Sample AK109 was collected in October 1997, and samples AK79, AK80, and AK81 were collected in May 1996.
[c] Collected from tributaries.

budget of several Himalayan rivers in Nepal because of the relatively low Sr concentration of the carbonates. This is also true to some extent in the Alaknanda, where the mean Sr concentration of the tributaries draining the Deoban Formation is only ~25 ng/g compared with ~50–60 ng/g of Sr in the main river. However, the very high $^{87}Sr/^{86}Sr$ ratio of the dissolved Sr means that the input has a disproportionate effect on the riverine $^{87}Sr$ flux and ultimately on seawater $^{87}Sr/^{86}Sr$ ratios. The impact of riverine Sr on seawater Sr isotope composition is proportional to both the flux of Sr carried and the difference between the $^{87}Sr/^{86}Sr$ ratio of the river and seawater (i.e., ~0.709). The increase in the $^{87}Sr/^{86}Sr$ ratio of the Alaknanda from ~0.728 to 0.735 as it flows across the outcrops of the Deoban Formation increases the forcing of the river on seawater $^{87}Sr/^{86}Sr$ ratios by ~35% without allowing for the increase in Sr flux over this section. Since tributaries drain mostly carbonate rocks over this section (fig. 2), it is probable that a significant fraction of the Sr is derived from the carbonate rocks.

Sr in Himalayan rivers is derived both from carbonate and silicate rocks from all three main tectonic units: the Tibetan Sedimentary Series, the High Himalayan Crystalline Series, and the Lesser Himalayan Series. In this study, we have demonstrated that the carbonates from both the High Himalayan Crystalline Series and the Lesser Himalayan Series have atypically high $^{87}Sr/^{86}Sr$ ratios as a result of exchange with silicate minerals during Himalayan and pre-Himalayan metamorphic events. The Tibetan Sedimentary Series carbonates have not been sampled, but it would not be surprising if their elevated $^{87}Sr/^{86}Sr$ ratios (e.g., Harris et al. 1998; Galy et al. 1999) were the result of metamorphic exchange with silicate minerals during the Himalayan metamorphism, which recrystallized the more deeply buried parts of the sequence.

It should be noted that the Alaknanda passes through a relatively extensive section of the Deoban Formation compared with the Bhagirathi and other tributaries in their joint catchment. Evaluation of the total impact of the extraordinarily high $^{87}Sr/^{86}Sr$ ratio carbonates on Himalayan river compositions will require budget estimates from a representative suite of rivers.

## Conclusions

Carbonate lithologies in both the High Himalayan Crystalline Series and the Lesser Himalaya have high $^{87}Sr/^{86}Sr$ ratios because many carbonates are relatively impure with high Rb/Sr ratios and because metamorphism and diagenesis has caused exchange of Sr between carbonate and silicates on scale lengths up to 0.5 m. The older and impure dolomitic calc-silicates with high Rb/Sr ratios from the Lesser Himalayas are both more abundant and have much higher $^{87}Sr/^{86}Sr$ ratios. Consequently, their dissolution has significant impact on the main river $^{87}Sr/^{86}Sr$ ratios despite their relatively low Sr contents.

Multiple diagenetic and metamorphic events have contributed to this exchange, including both the high- and low-grade Himalayan events. Exhumation of these rocks is a consequence of the Himalayan orogeny, and it is tempting to speculate that collisional orogenic events will tend to expose such metamorphosed carbonate rocks with elevated $^{87}Sr/^{86}Sr$ ratios and thus that the episodicity in the seawater Sr isotopic record is forced by collisional orogens. However, although the extremely high $^{87}Sr/^{86}Sr$ carbonates contribute to the elevated riverine Sr isotopic compositions, they only contribute part of the flux of elevated $^{87}Sr/^{86}Sr$ strontium; the rest is derived from silicate lithologies or finely dispersed carbonate within silicate rocks (cf. Blum et al. 1998). Careful assessment of the total budget of the Himalayan rivers is required before the sources and fluxes of $^{87}Sr$ from the Himalayas can be properly determined.

### ACKNOWLEDGMENTS

J. Trivedi and S. Krishnaswami are thanked for their comments on an early draft of the article. This research was supported by the United Kingdom Natural Environment Research Council.

### REFERENCES CITED

Ahmad, T.; Harris, N.; Bickle, M.; Chapman, H.; Bunbury, J.; and Prince, C. 2000. Isotopic constraints on the structural relationships between the Lesser Himalayan Series and the High Himalayan Crystalline Series, Garhwal Himalaya. Geol. Soc. Am. Bull. 112: 467–477.

Banner, J. L. 1995. Application of the trace element and isotope geochemistry of strontium to studies of carbonate diagenesis. Sedimentology 42:805–824.

Bickle, M. J. 1994. The role of metamorphic decarbonation reactions in returning strontium to the silicate sediment mass. Nature 367:699–704.

———. 1996. Metamorphic decarbonation, silicate weathering and the long-term carbon cycle. Terra Nova 8:270–276.

Bickle, M. J., and Chapman, H. J. 1990. Strontium and oxygen isotope decoupling in the Hercynian Trois Seigneurs massif, Pyrenees: evidence for fluid circulation in a brittle regime. Contrib. Mineral. Petrol. 104:332–347.

Bickle, M. J.; Chapman, H. J.; Ferry, J. M.; Rumble, D., III; and Fallick, A. E. 1997. Fluid-flow and diffusion in the Waterville Limestone, south-central Maine: constraints from strontium, oxygen and carbon isotope profiles. J. Petrol. 38:1489–1512.

Bickle, M. J.; Chapman, H. J.; Wickham, S. M.; and Peters, M. T. 1995. Strontium and oxygen isotope profiles across marble-silicate contacts, Lizzies Basin, East Humbolt Range, Nevada: constraints on metamorphic fluid flow. Contrib. Mineral. Petrol. 121:400–413.

Blum, J. D.; Gazis, C. A.; Jacobson, A. D.; and Chamberlain, C. P. 1998. Carbonate versus silicate weathering in the Raikhot watershed within the High Himalayan Crystalline Series. Geology 26:411–414.

Bunbury, J.; Bickle, M.; Ahmad, T.; Fairchild, I.; Harris, N.; and Chapman, H. 2000. Experiments to investigate the contribution of silicate weathering to the dissolution of Himalayan rocks. Goldschmidt 2000 Conference, Oxford. J. Conf. Abstr. 5:265.

Derry, L. A., and France-Lanord, C. 1996. Neogene Himalayan weathering history and river $^{87}Sr/^{86}Sr$ impact on the marine Sr record. Earth Planet. Sci. Lett. 142: 59–74.

Edmond, J. M. 1992. Himalayan tectonics, weathering processes, and the strontium isotope record in marine limestones. Science 258:1594–1597.

English, N. B.; Quade, J.; DeCelles, P. G.; and Garzione, C. 2000. Geologic control of Sr and major element chemistry in Himalayan rivers, Nepal. Geochim. Cosmochim. Acta 64:2549–2566.

France-Lanord, C.; Derry, L.; and Michard, A. 1993. Evolution of the Himalaya since Miocene time: isotopic and sedimentological evidence from the Bengal fan. *In* Treloar, P. J., and Searle, M. P., eds. Himalayan tectonics. Geol. Soc. Lond. Spec. Publ. 74:603–621.

Gairola, V. K. 1975. On the petrology and structure of the central crystallines of the Garhwal Himalaya, Uttar Pradesh. Himalayan Geol. 4:455–472.

Galy, A.; France-Lanord, C.; and Derry, L. A. 1999. The strontium isotopic budget of Himalayan Rivers in Nepal and Bangladesh. Geochim. Cosmochim. Acta 63: 1905–1925.

Harris, N. B. W. 1995. Significance of weathering of Himalayan metasedimentary rocks and leucogranites for the Sr isotope evolution of seawater during the Miocene. Geology 23:795–798.

Harris, N. B. W.; Bickle, M. J.; Chapman, H. J.; Fairchild, I.; and Bunbury, J. 1998. The significance of Himalayan rivers for silicate weathering rates: evidence from the Bhoti Kosi tributary. Chem. Geol. 144:205–220.

Harrison, T. M.; Ryerson, F. J.; Le Fort, P.; Yin, A.; Lovera, O. M.; and Catlos, E. J. 1997. A Late Miocene-Pliocene origin for the central Himalayan inverted metamorphism. Earth Planet. Sci. Lett. 146:E1–E7.

Hodges, K. V.; Burchfiel, B. C.; Royden, L. H.; Chen, Z.; and Liu, Y. 1993. The metamorphic signature of contemporaneous extension and shortening in the central Himalayan orogen: data from the Nyalam transect, southern Tibet. J. Metamorph. Geol. 11:721–737.

Inger, S., and Harris, N. B. W. 1992. Tectonothermal evolution of the High Himalayan Crystalline Sequence, Langtang Valley, Northern Nepal. J. Metamorph. Geol. 10:439–452.

Jacobsen, S. B., and Kaufman, A. J. 1999. The Sr, C and O isotopic evolution of Neoproterozoic seawater. Chem. Geol. 161:37–57.

Krishnaswami, S., and Singh, S. K. 1998. Silicate and carbonate weathering in the drainage basins of the Ganga-Ghaghara-Indus head waters: contributions to major ion and Sr isotope geochemistry. Proc. Indian Acad. Sci. Earth Planet. Sci. 107:283–291.

Krishnaswami, S.; Singh, S. K.; and Dalai, T. K. 1999. Silicate weathering in the Himalayas: role in contributing to major ions and radiogenic Sr to the Bay of Bengal. *In* Somayajulu, B. L. K., ed. Ocean science: trends and future directions. New Delhi, Indian National Science Academy and Akademi Book International, p. 23–51.

Krishnaswami, S.; Trivedi, J. R.; Sarin, M. M.; Ramesh, R.; and Sharma, K. K. 1992. Strontium isotopes and rubidium in the Ganga-Brahmaputra river system: weathering in the Himalaya, fluxes to the bay of Bengal and contributions to the evolution of oceanic $^{87}Sr/^{86}Sr$. Earth Planet. Sci. Lett. 109:243–253.

Kumar, S., and Tewari, V. C. 1978. Occurrence of *Conophyton gargariens* from the Gangolihat Dolomite, Kathpuria China area, Almora District, U.P. J. Geol. Soc. India 19:174–178.

Le Fort, P. 1975. Himalayas: the collided range: present knowledge of the continental arc. Am. J. Sci. 275A: 1–44.

Metcalfe, R. P. 1990. A thermotectonic evolution for the Main Central Thrust and higher Himalaya, Western Garhwal, India. Ph.D. thesis, University of Leicester, 194 p.

———. 1993. Pressure, temperature and time constraints on metamorphism across the Main Central Thrust Zone and High Himalayan Slab in the Garhwal Himalaya. *In* Treloar, P. J., and Searle, M. P., eds. Himalayan tectonics. Geol. Soc. Lond. 74:485–509.

Misra, R. C., and Sharma, R. P. 1973. Geology of the Nandprayag klippe and central Crystallines, Kamaun Himalayas. Bull. Indian Geol. Assoc. 6:85–98.

Oliver, G. J. H.; Johnson, M. R. W.; and Fallick, A. E. 1995. Age of metamorphism in the Lesser Himalaya and the Main Central Thrust Zone, Garhwal India: results of illite crystallinity, $^{40}Ar$-$^{39}Ar$ fusion and K-Ar studies. Geol. Mag. 132:139–149.

Palmer, M. R., and Edmond, J. M. 1992. Controls over the strontium isotope composition of river water. Geochim. Cosmochim. Acta 56:2099–2111.

Parrish, R. P., and Hodges, K. V. 1996. Isotopic constraints

on the age and provenance of the Lesser and Greater Himalayan sequences. Geol. Soc. Am. Bull. 108: 904–911.

Prince, C. I. 1999. The timing of prograde metamorphism in the Garhwal Himalaya, India. Ph.D. thesis, Open University, Milton Keynes, 308 p.

Quade, J.; Roe, L.; DeCelles, P. G.; and Ojha, T. P. 1997. The Late Neogene $^{87}Sr/^{86}Sr$ record of lowland Himalayan rivers. Science 276:1828–1831.

Raymo, M. E., and Ruddiman, W. F. 1992. Tectonic forcing of Late Cenozoic climate. Nature 359:117–122.

Raymo, M. E.; Ruddiman, W. F.; and Froelich, P. N. 1988. Influence of Late Cenozoic mountain building on ocean geochemical cycles. Geology 16:649–653.

Richter, F. M.; Rowley, D. B.; and DePaolo, D. J. 1992. Sr isotope evolution of seawater: the role of tectonics. Earth Planet. Sci. Lett. 109:11–23.

Singh, S. K.; Trivedi, J. R.; Pande, K.; Ramesh, R.; and Krishnaswami, S. 1998. Chemical and strontium, oxygen, and carbon isotopic compositions of carbonates from the Lesser Himalaya: implications to the strontium isotope composition of the source waters of the Ganga, Ghaghara, and the Indus Rivers. Geochim. Cosmochim. Acta 62:743–755.

Srivasta, P., and Mitra, G. 1994. Thrust geometries and deep structure of the outer and Lesser Himalaya: implications for evolution of the Himalayan fold-and-thrust belt. Tectonics 13:89–109.

Thakur, V. C., and Rawat, B. S. 1992. Geological map of Western Himalaya. Dehra Dun, India, Wadia Institute of Himalayan Geology, scale 1 : 1,000,000.

U.S. Army Corps of Engineers. 1954. Army Map Service Series U502. Washington, D.C., U.S. Army, scale 1 : 250,000.

Valdiya, K. S. 1980. Geology of Kumaun Lesser Himalaya. Dehra Dun, India, Wadia Institute of Himalayan Geology, 291 p.

———. 1995. Proterozoic sedimentation and Pan-African geodynamic development in the Himalaya. Precambrian Res. 74:35–55.

Vance, D., and Harris, N. 1999. Timing of prograde metamorphism in the Zanskar Himalaya. Geology 27: 395–398.

Veizer, J. 1989. Strontium isotopes in seawater through time. Annu. Rev. Earth Planet. Sci. 17:141–167.

Yoo, C. M.; Greg, J. M.; and Shelton, K. L. 2000. Dolomitization and dolomite neomorphism: Trenton and Black River Limestones (Middle Ordovician) Northern Indiana, USA. J. Sediment. Res. 70:265–274.

York, D. 1969. Least squares fitting of a straight line with correlated errors. Earth Planet. Sci. Lett. 5:320–324.